ARMY RESEARCH LABORATORY

UXO Detection Using Optical Sensors

by Dale E. Robinson and William C. Ruff

ARL-MR-226

October 1997

The findings in this report are not to be construed as an official Department of the Army position unless so designated by other authorized documents.

Citation of manufacturer's or trade names does not constitute an official endorsement or approval of the use thereof.

Destroy this report when it is no longer needed. Do not return it to the originator.

Army Research Laboratory
Adelphi, MD 20783-1197

ARL-MR-226 **October 1997**

UXO Detection Using Optical Sensors

Dale E. Robinson and William C. Ruff
Sensors and Electronic Devices Directorate

sponsored by
Test and Evaluation Command
Yuma Proving Ground, AZ 85365

Abstract

Owing to cuts in the Defense Department budget, many military bases have been forced to close. Before these bases can be converted from military to civilian use, the unexploded ordnance (UXO) must be located and completely removed. The ordnance to be cleaned ranges from large-caliber rounds to small submunitions, which can be as small as 2 cm in diameter. In this report, we derive the basic theory necessary for the design of a UXO sensor operating in the visible to far-infrared wavelength regions. We then analyze several commercial off-the-shelf (COTS) sensors that could be used for UXO detection and present a few general conclusions on work required before a UXO sensor is fabricated.

Contents

Figures

Tables

1. Introduction

Owing to cuts in the Defense Department budget, many military bases have been forced to close. Before these bases can be converted from military to civilian use, the unexploded ordnance (UXO) and waste must be completely removed. The ordnance to be cleaned ranges from large-caliber rounds to small submunitions. The submunitions can be as small as 2 cm in diameter. Yuma Proving Ground in Arizona has been chosen as a testbed for this problem.

One solution to the UXO removal problem is multi-sensor fusion including some or all of the following sensors: magnetometer, ground penetration radar, millimeter wave radiometer, ladar, visible imager, and infrared (IR) imager. The data from each of these sensors are to be integrated and registered. The purpose of this report is to show that an IR/visible sensor can be used to detect surface UXO as small as 2 cm in diameter.

2. General Background

2.1 Visible to Near Infrared (Nonthermal)

The detection of an object in the visible to near infrared (NIR) spectral region depends on two parameters: the object's reflectance characteristics and the source of illumination used for the measurement. The sun is used as the illumination source for most visible-to-NIR systems, photographic systems, etc, although it is also possible to use other light sources, such as a laser. An object's reflectance is its primary signature component and varies with the physical condition of the object (surface roughness, water content, etc), the angle between the measurement device and the object's surface normal, the angle between the illumination source and the object's surface normal (except for perfectly diffuse reflectors), and the wavelength band in which the measurement is performed. For instance, it is the spectral reflectance variation that gives an opaque object its characteristic color in the visible portion of the spectrum; i.e., an apple looks red because of its high reflectance in the red portion of the visible spectrum relative to the other colors.

The two distinctive angular reflectance characteristics of a material are known as specular and diffuse reflectance. A specular reflection gives a material a mirror-like appearance and occurs when the angle of the measurement relative to the object's surface normal is equal to the angle of the illumination source relative to the object's surface normal, as shown in figure 1. This effect tends to wash out the object's natural color (its diffuse reflectance). For example, just after a car has been waxed and polished, especially a dark colored car, it is sometimes difficult to determine the color of the car because of the intense, mirror-like reflections of the surrounding background.

A diffuse reflection, on the other hand, scatters the illuminating light equally in all directions, as shown in figure 2. Surfaces with purely diffuse reflection characteristics are known as Lambertian surfaces. Most objects exhibit both specular and diffuse reflectance characteristics, although it is possible for very rough objects to have only a diffuse reflectance and for very smooth objects, like glass, to have only a specular reflectance.

A general expression for the reflectance coefficient, ρ, requires the measurement of both the incident and scattered flux at all angles surrounding the sample. This is expressed as

$$\rho = \left. \frac{L_r \partial \Omega_r}{L_i \partial \Omega_i} \right|_{\Omega_i \Omega_r} ,$$

where $L_{i,r}$ is the incident and reflected irradiance over the projected incremental solid angle $\partial\Omega$. This expression takes into account the variation of the reflectance over all angles and represents objects that exhibit specular, diffuse, and mixed characteristics. This definition requires the solid angles Ω_i and Ω_r used for the measurement to be specified along with the reflectance value. The bidirectional reflectance distribution function (BRDF, in units of sr^{-1}) is a differential quantity used to specify the reflectance value over the hemisphere surrounding the sample:

$$\rho_{bd} \equiv \frac{L_r}{L_i \partial \Omega_i} .$$

Figure 1. Specular reflection.

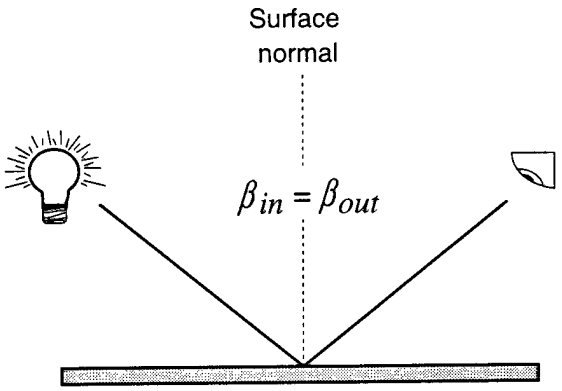

Figure 2. Diffuse reflection.

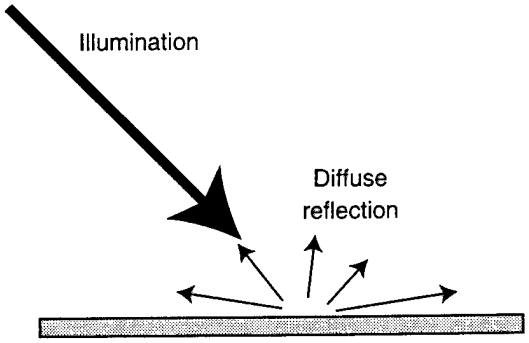

The directional reflectance, ρ_d, is defined as the BRDF integrated over a hemisphere and normalized to unity for a perfect (lossless) Lambertian surface. For a Lambertian reflector, ρ_d is

$$\rho_d = \int_{hemisphere} \rho_{bd} \partial\Omega = \pi \rho_{bd} \ .$$

It is the directional reflectance that is used in the conservation of energy equations relating ρ and emissivity, ε (discussed in the following sections).

In some cases, such as field measurements, the angular variation along the θ direction is measured, and it is assumed that the reflectance of the sample is independent of the ϕ direction. For Lambertian reflectors,

$$\rho_{fm} = \pi \cos\theta \, \rho_{bd} \ .$$

A normalization constant of $\rho_0 = \rho_{fm}\big|_{\theta=0}$ is used to simplify the equation, and like the directional reflectance above, the reflectance is normalized to unity for a perfect Lambertian surface. For such a reflector, $\rho_{bd} = 1/\pi$. The angular dependence in the above equation is due solely to the geometry of the measurement: i.e., the apparent area of the object decreases as θ increases. Unlike the specular reflectance, the diffuse reflectance of a material can be exactly calculated given that the value of ρ_0 can be found. This is important for modeling the performance of a sensor. The value of ρ_{fm} is typically given as a percentage, with the maximum of 100 percent defined as the reflectance of a perfect Lambertian standard (set by the National Institute of Standard and Technology—NIST) measured at normal incidence.

Figure 3 is an example of the reflectance, ρ_{fm}, versus angle of a painted metal surface measured under three different surface conditions. The material sample is an olive drab painted aluminum fuselage panel, measured on an operational military helicopter. The sample appeared glossy to the eye and was probably polished, along with the rest of the aircraft, to

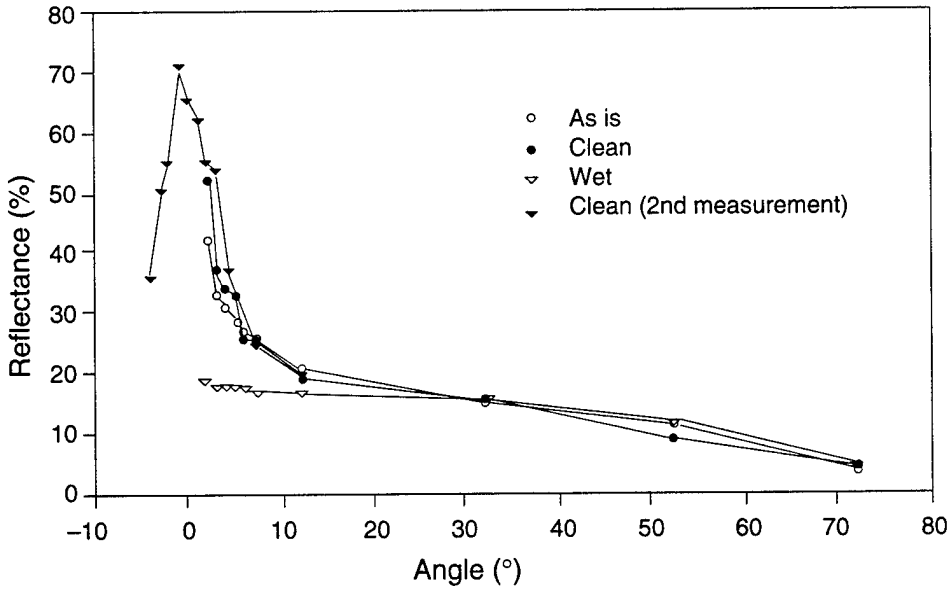

Figure 3. Reflection versus angle of illumination for a partial aluminum panel under three conditions.

decrease the aircraft's aerodynamic drag. The reflectance was measured at a wavelength of 0.9 μm with a GaAs semiconductor laser diode as an illumination source. The sensor used has an independent transmitter and receiver lens assembly, separated in angle by a few degrees at the measurement point. The reflectance was measured for three separate surface conditions: the surface as it was found; the surface wet with a light mist; and the surface cleaned with an alcohol solution. The clean surface was measured a second time, with more points collected around the surface normal.

The panel measurements demonstrate specular reflectance characteristics at angles around 0 ± 10° and diffuse reflectance characteristics at angles greater than 10°. Normal incidence corresponds to 0° on the plot. The specular reflectance, occurring at near normal incidence, achieves a peak value of approximately 70 percent and a full width at half maximum of nearly 10°. The specular reflectance does change with surface condition, but because of the limited number of points taken near normal incidence, the amount of change is hard to quantify. The diffuse reflectance value for this panel at normal incidence is approximately 20 percent, with the value slowly decreasing with measurement angle.

It is possible, because of the way the reflectance coefficient is defined, for a specular reflection to peak above 100 percent. This would represent a case where more energy is reflected from the surface in the specular peak than that scattered from a 100-percent diffuse target, which scatters the energy equally into a hemisphere.

The reflectance of a material also varies with wavelength. This variation is due to the molecular interaction of the object with the incident radiation at the surface level for opaque materials, or throughout the object for translucent materials. A generalized directional reflectance curve for a green leaf, shown in figure 4 [1], is plotted versus wavelength. A description of the phenomena affecting the reflectance in different spectral regions is also given in the figure. For example, the high reflectance around 1.0 μm is due to the high reflectance of the chlorophyll molecules in the leaf, while the

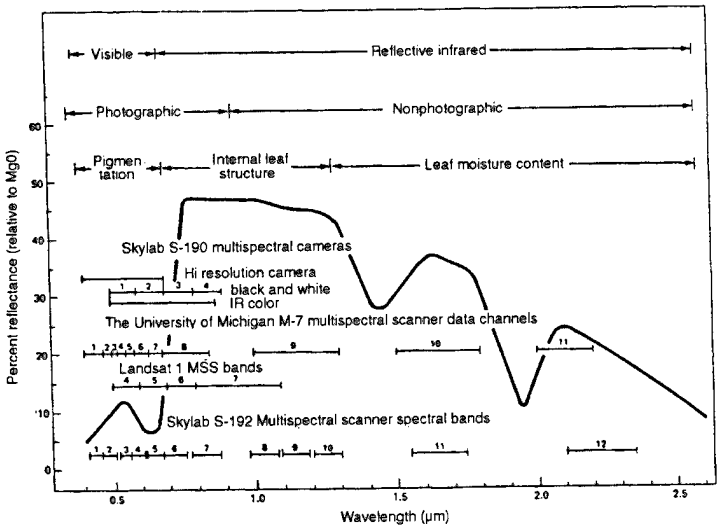

Figure 4. Generalized directional reflectance curve of a green leaf (used with permission, Lintz and Simonett [1]).

low-reflectance regions around 1.5 and 2.0 μm are due to the high absorption of the water in the leaf at these wavelengths. This effect can be an advantage if spectral regions of high contrast can be found between the UXO and the surrounding background. For instance, the "day-glow" orange color used by hunters assists in avoiding hunting accidents by aiding in the identification of the hunter and the prey. Even in dense woods where a hunter may be mostly obscured, portions of the orange may be easily discernible (meaning you probably shouldn't shoot).

The source of the illumination used to make a measurement must also be considered: its spectral characteristics, intensity, polarization properties, location with respect to the object and the measurement device, and related shadowing effects. The primary illumination source used for visible and NIR systems is the sun. We can approximate the irradiance of the sun at sea level by calculating the irradiance from a blackbody radiator at a temperature of 5900 K (the apparent temperature of the sun) and filtering this radiation through the atmosphere. The atmospheric constituents CO_2, H_2O, etc, preferentially absorb specific wavelength bands, giving the solar irradiance blackbody curve its spectral detail. Figure 5 [2] is a plot of the solar irradiance versus wavelength measured at sea level and outside the atmosphere, along with an indication of the various atmospheric absorption bands. We need this information when selecting a wavelength band for a passive system to operate in (i.e., a passive measurement system operating at an absorption band would not be practical for UXO detection).

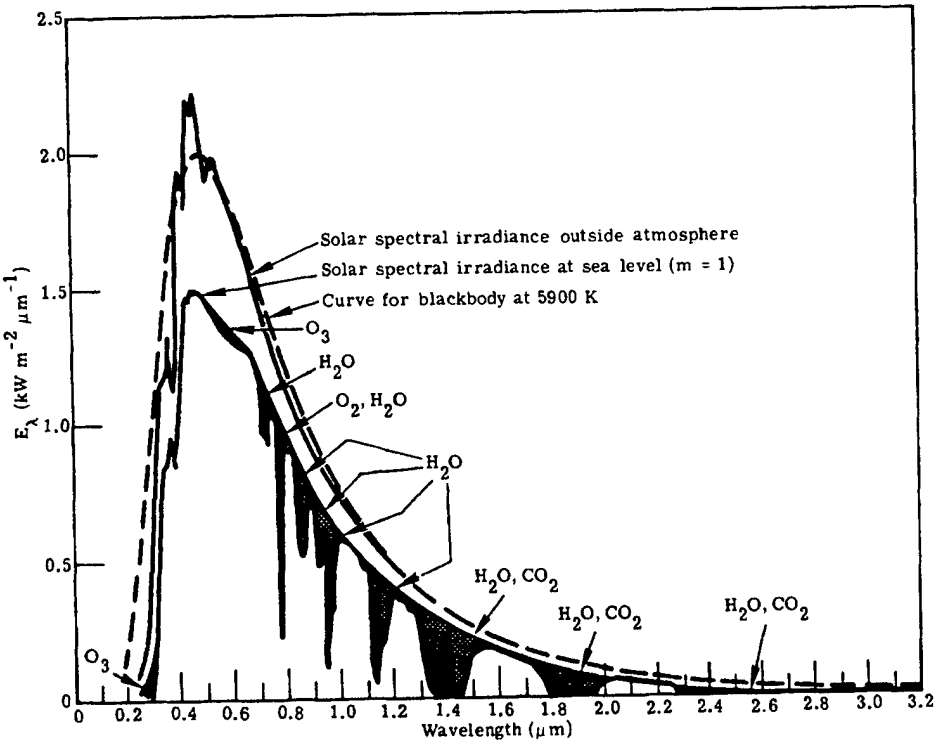

Figure 5. Spectral distribution curves related to sun. Shaded areas indicate absorption at sea level (Wolfe and Zissis [4]).

Selection of the time of day is also crucial for making a passive measurement. The solar zenith angle (angle of the sun above the horizon) determines the amount of atmosphere the light needs to pass through, and therefore the degree of atmospheric absorption. This angle also determines the amount of shadowing in the scene. For small zenith angles (sun at high noon), the amount of atmosphere and the shadowing visible in a scene are at a minimum. This is usually optimal for passive detection of objects on the ground. Under some cases of UXO detection, however, it may be advantageous to operate the system when the sun is close to the horizon. Under this condition, a small object in the scene will cast a large shadow, which may be easier to detect than the object itself.

Lasers can also be used as an illumination source. Typically, a laser can provide coherent radiation with a known polarization and intensity. It may be possible to select a laser line in a spectral band where the contrast is high between the UXO and the background. Also, man-made objects tend to depolarize light less than natural objects, such as grasses, earth, etc, and therefore it may be possible to discriminate between UXO and background based on the reflected light's polarization [3].

2.2 Thermal Infrared

In the thermal IR region, an object's thermally emitted radiation properties are measured, and therefore (unlike in the visible to NIR) no illumination is required. The amount of radiation emitted from an object depends on two parameters, the temperature and emissivity of the object. We related the emissivity of an object to its directional reflectance, using conservation of energy, by

$$\rho_d + \varepsilon + \tau = 1 \ ,$$

where ρ_d is as defined previously, and ε and τ are the material's emissivity and transmittance, respectively. For opaque materials, the transmittance of the material is equal to zero, leaving

$$\varepsilon = 1 - \rho_d \ .$$

Like the directional reflectance, the emissivity of an object is a function of its physical condition (surface roughness, water content, etc) and the wavelength band in which the measurement is performed.

The temperature of natural surface objects is controlled mainly by the diurnal cycle. During this cycle, objects warm up during the day from solar radiation and cool at night by radiation into the atmosphere. The rate of change in temperature of an object depends on many factors, such as emissivity, size, shape, heat capacity, conductivity, and conduction/convection effects, as shown in figure 6 [1]. The combination of these effects is referred to as the solar load. Solar loading differences among materials cause a temperature contrast between an object and the background that is detectable by a thermal detector. Metallic objects typically have a higher solar load than the natural background scene. This contrast between the desired target and the background will be greatest just after sunrise and just after

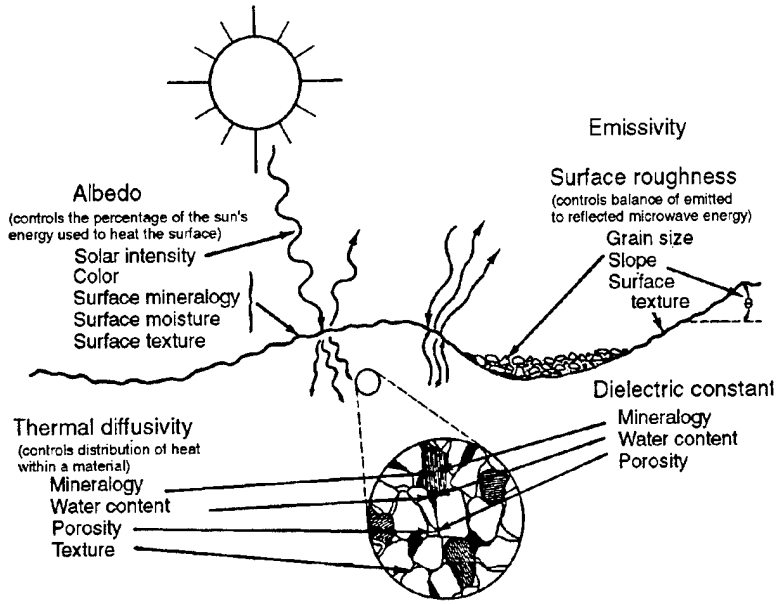

Figure 6. Solar loading diagram (used with permission, Lintz and Simonett [1]).

sunset. This contrast difference arises because the background warms faster than the object at sunrise and cools faster at sunset.

The spectrum of radiation emitted by a warm object may be calculated by Planck's equation. In order to estimate the expected radiant exitance of both targets and backgrounds, we assume that the surfaces emit radiation diffusely (refer to fig. 2 and omit the illumination source). Therefore, these surfaces can be considered Lambertian. The power radiated per unit wavelength by a Lambertian blackbody source, given by Planck's equation, in terms of spectral radiant exitance (in watts per meters squared) is

$$M_{bb}(\lambda,T) = \frac{2\pi c^h}{\pi^5} \frac{1}{e^{cg/\lambda kT} - 1} ,$$

where

c = the speed of light (2.998×10^8 m/s),

h = Planck's constant (6.626×10^{-34} J–s),

k = Boltzmann's constant (1.3806×10^{-23} J–K^{-1}),

λ = wavelength, and

T = temperature (K).

Since neither the background nor the ordnance is a pure blackbody, the spectral radiant exitance must be multiplied by the spectral emissivity. The emissivity is defined as the ratio of the radiance of a body to that of an ideal blackbody:

$$M(\lambda) = \varepsilon(\lambda)\, M_{bb}(\lambda) .$$

The apparent temperature of an object is the temperature calculated from the spectrum of radiation that the body emits, with the assumption that $\varepsilon = 1$. This measured temperature differs from the body's true temperature if the emissivity of the object is not unity.

3. Signatures

Ground truth data (i.e., reflectance and emissivity measurements) for a test area at YPG are currently being collected. Although these data were not available at the time of writing, estimates of the reflectance and emissivity characteristics of the UXO and surrounding backgrounds were made from other sources and are presented below.

3.1 Visible to Near Infrared (Nonthermal)

It is not difficult to design an optical sensor that can detect UXO on the surface. In fact, a number of commercial systems are already available that can do the job. The difficulty with UXO remediation, however, will be in discriminating the UXO among the thousands of acres of rocks, vegetation, soda cans, and other man-made and natural clutter. It is therefore imperative that the reflectance properties of the UXO and clutter background be fully characterized and understood before a commitment is made to a particular optical sensor suite. This has not yet been done, although some measurements are in the process of being made. In this section, we explain several photographs and some data using the general reflectance phenomenology outlined in the previous section, along with discussions on how the phenomenology applies to UXO detection.

Figure 7 is a photograph of the Kofa test range at Yuma Proving Ground, taken in the spring of 1992. This test range is fairly flat with light elevation rolls and is sparsely populated with vegetation in the form of bushes and at least one cactus. The color in the photograph makes it easy to discriminate between the green vegetation and the lightly colored, sandy soil. A few of the instruments in the scene stand out in the photo because of their highly specular reflection of the sunlit sky. Painted UXO or attachments to UXO, such as parachutes, could also be discriminated easily. Small shadows are visible near the bushes, indicating that the scene was photographed when the sun was near noon.

Figure 8 [1] is a photograph of citrus groves near Mesa, AZ, spanning the visible to NIR wavelengths. The leafy vegetation is clearly evident because of its high NIR reflectance characteristics. It should be easy to use this reflectance characteristic to discriminate between leafy vegetation and unpainted surface UXO. On the other hand, some military paints emulate the high-NIR reflectance characteristics of leafy plants for camouflage purposes, so this discrimination technique will not work in all cases.

Recall that the directional reflectance of a generic green leaf was plotted in figure 4. Figures 9 to 12 give the directional reflectance characteristics for various materials in the visible and NIR bands. Figure 9 [4], which includes data in the thermal IR band, plots the spectral reflectance characteristics of soils taken from various locations. Figures 10 and 11 [4] show plots of the directional reflectance characteristics of a number of different rock types and of sagebrush and yucca plants, respectively. Figure 12 [3] is a plot of the directional reflectance characteristics for a couple of scatterable mine types, background, and vegetation. Each material has its own unique characteristic which, if known in advance, may aid in discriminating among rocks, soil, plants, and surface UXO.

Figure 7. YPG Kofa test range (photograph taken in spring of 1992.)

Figure 8. Photograph of citrus groves near Mesa, AZ, in visible to NIR wavelength bands (used with permission, Lintz and Simonett [1]).

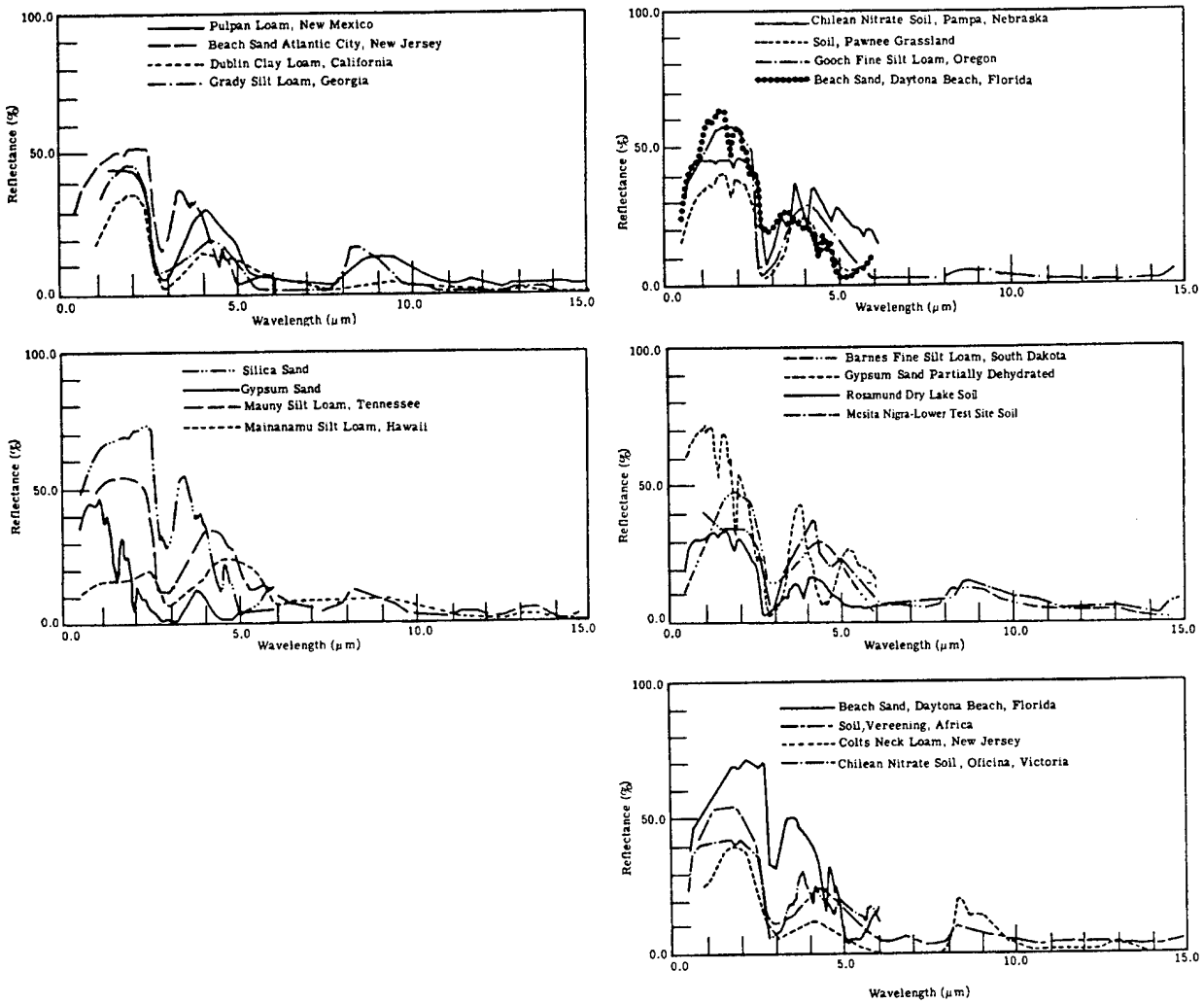

Figure 9. Characteristic directional reflectance of various soils (Wolfe and Zissis [4]).

Figure 10. Spectral reflectance of common rock types (Wolfe and Zissis [4]).

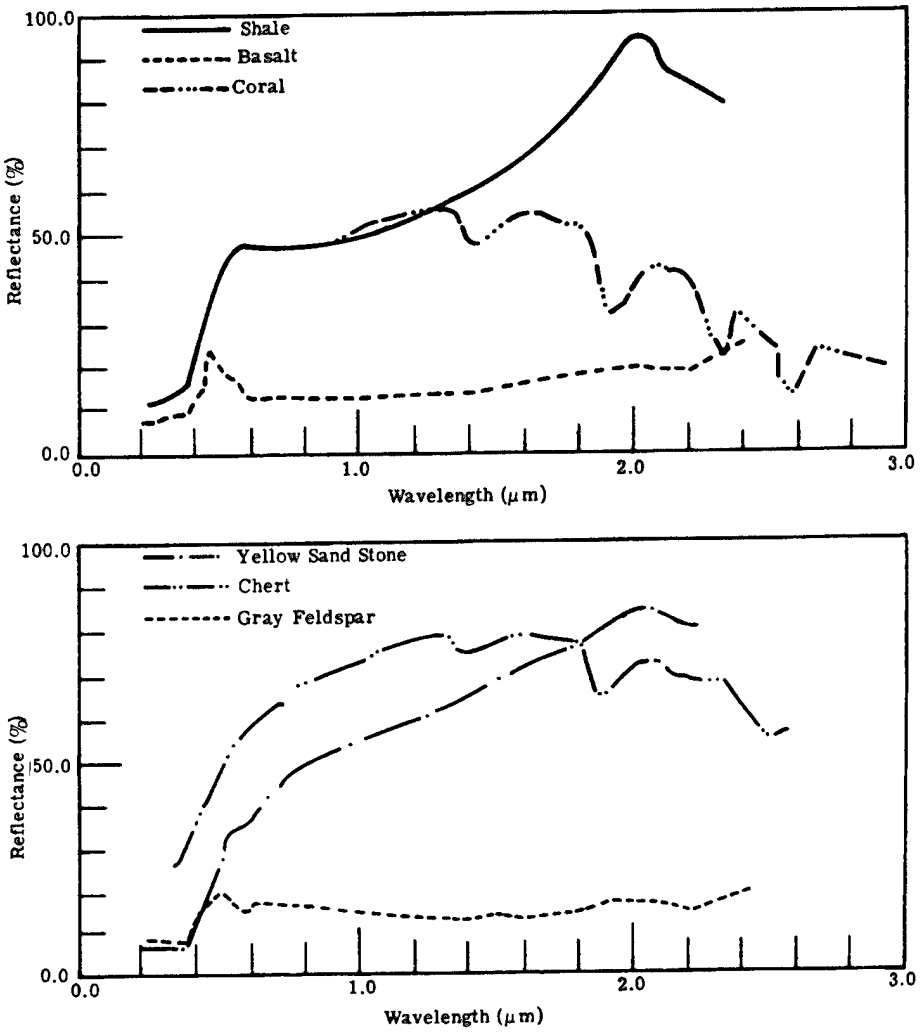

Figure 11. Characteristic reflectance of sagebrush and yucca (Wolfe and Zissis [4]).

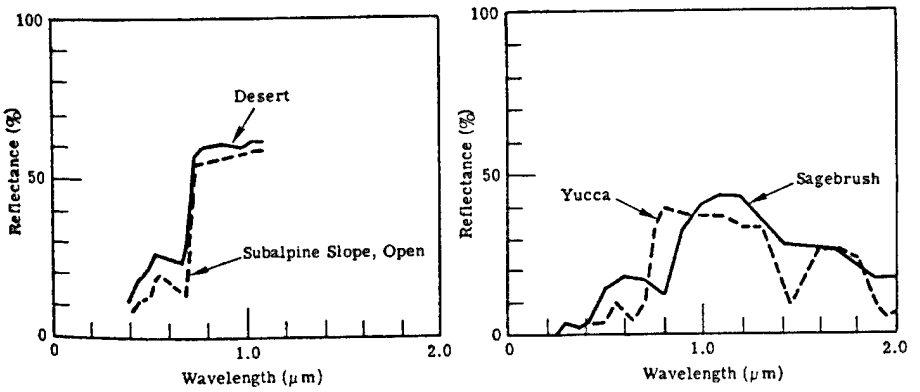

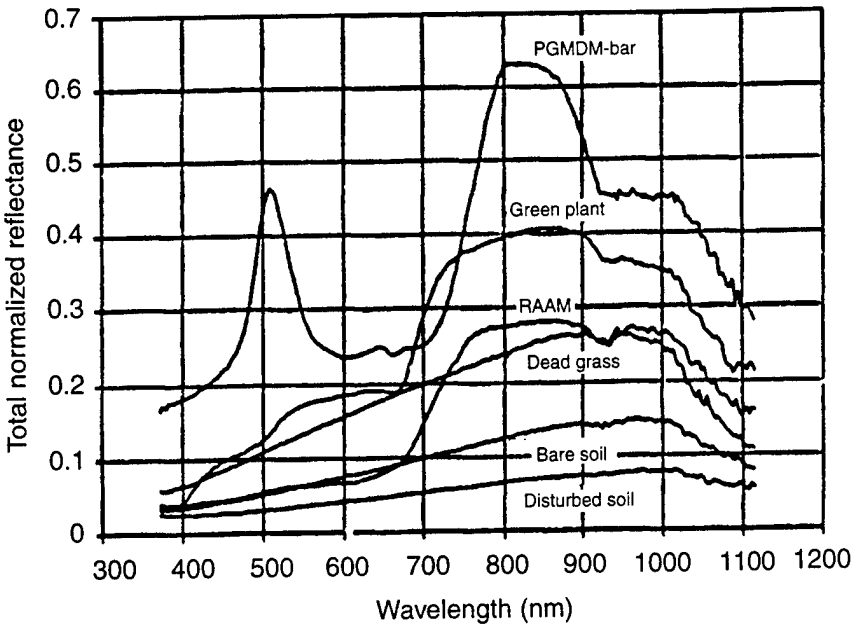

Figure 12. Directional reflectance for scatterable mine types and various backgrounds (Ballard et al [3]).

3.2 Thermal Infrared

Although no spectral emissivity data are available for the sand and rocks of Yuma, AZ, figure 9 shows the directional reflectance of different sands and soils for wavelengths up to 15 μm. We can calculate the emissivity from the reflectance curves, using $\varepsilon = 1 - \rho_d$ and assuming that the material is opaque. It is assumed that the background contains not only sand and rocks, but also some vegetation. This vegetation is mainly in the form of brush, sagebrush, and cactus.

The unexploded ordnance that is to be detected is assumed to be made up of various painted and raw metals and plastics, although the exact materials are unknown. Since the ordnance is assumed to be scattered on the surface and exposed to the environment, the metallic surfaces may be oxidized. Some insight concerning the emissivities expected to be characteristic of the ordnance may be gained from the total (i.e., spectrally integrated) normal emissivities of some man-made materials, which are shown in table 1. Hudson [5], who gives the emissivity information, does not explicitly state the measurement spectral band. However, the data may be inferred from Hudson to be valid in the IR region.

An NIR sensor relies on the reflectance differences between the target and the background scene for detection. However, emissivity differences do not provide sufficient contrast for thermal imagers. As shown in table 1 and figures 9 and 13 [4], there is not a strong emissivity difference between oxidized metals and the desert sand. The emissivity of sand is ≈0.7 from 3 to 5 μm and ≈0.95 from 8 to 12 μm. The emissivity of iron oxide, as shown in table 1 and figure 13, is ≈0.9 for both the 3- to 5-μm and 8- to 12-μm ranges. Thus the thermal detector must rely on solar loading for detection, as described in section 2.2. In the desert environment, the solar load of ordnance is larger than the load of sand and vegetation. However, the solar load of larger, dense rocks may be comparable to the load of the ordnance and may cause some false alarms. The false-alarm rate can be reduced when the imager functions with other sensor types.

Table 1. Emissivity of various man-made objects (Wolfe and Zissis [4], Hudson [5], and ERIM [6]).

Metals and their oxides	Temperature (°F)	Emissivity (IR region[a])	Emissivity (9.3 μm)
Aluminum: Polished sheet	100	0.05	0.04
Sheet as received	100	0.09	—
Anodized sheet, chromic acid process	100	0.55	—
Vacuum deposited	20	0.04	—
Oxidized	100	—	0.11
Brass: Highly polished	100	0.03	0.1
Rubbed with 80-grit emery	20	0.20	—
Oxidized	100	0.61	0.61
Copper: Polished	100	0.05	0.04
Heavily oxidized	20	0.78	0.87
Gold: Highly polished	100	0.02	—
Iron: Cast, polished	40	0.21	0.06
Cast, oxidized	100	0.64	0.63
Sheet, heavily rusted	20	0.69	—
Sheet, heavily rusted	100	—	0.96
Magnesium: Polished	20	0.07	—
Polished	100	—	0.07
Nickel: Electroplated, polished	20	0.05	—
Electroplated, no polish	20	0.11	—
Oxidized	200	0.37	—
Silver: Polished	100	0.03	—
Stainless-steel: Type 18-8 buffed	20	0.16	—
Type 18-8, oxidized at 800°C	60	0.85	—
Steel: Polished	100	0.07	—
Oxidized	100	—	0.79
Oxidized	200	0.79	—
Tin: Commercial tin-plated sheet iron	100	0.07	—
Other materials	—	—	—
Brick: Red common	20	0.93	—
Oil, lubricating (thin film on nickel base):	—	—	—
Nickel base alone	20	0.05	—
Film thickness 0.001, 0.002, 0.005 in.	20	0.27, 0.46, 0.72	—
Thick coating	20	0.82	—
Paint, oil: Average of 16 colors	100	0.94	—
Sand	20	0.90	—
Soil: Dry	20	0.92	—
Saturated with water	20	0.95	—

[a]*Wavelength range not specified.*

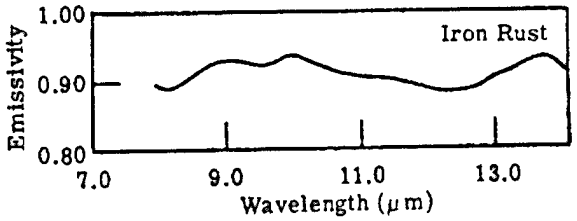

Figure 13. Emissivity of iron rust (Wolfe and Zissis [4]).

4. Example Sensors and Paint

This section presents sensors and an experimental paint (currently available off the shelf) that, with some modifications, may be used for the detection or characterization of surface UXO. We also present an experimental paint that, with the proper laser illuminator, could be useful for tagging future ordnance. The sensors and paint span the visible through the thermal IR spectral region and exploit the phenomena discussed in the previous sections. The list should not be considered exhaustive, and, as study continues, other sensors, as they appear viable, should be evaluated.

4.1 Spectroscopic Camera (Visible to NIR)

The stereoscopic camera (see table 2), like any camera, displays the reflectance differences of a scene using the sun as an illumination source. These data are digitized, with each pixel mapped to an x, y, z (height) and reflectance value and stored for further analysis. Currently, the camera uses black and white film and operates over the entire spectral band from visible to NIR. However, the camera can be fitted with spectral filters, and by using multiple, registered cameras on the same airborne platform, one could collect multiband spectral data. As a first cut, four spectral regions are suggested: red, green, and blue (RGB) to generate high-resolution color images for discriminating painted UXO and UXO with attached colored parachutes, and NIR to aid in the discrimination of plant life.

Table 2. Features of spectroscopic camera.

Feature	Description
Sensor type	Stereoscopic photography
Spectral bands:	
Current	Visible & NIR
Suggested	Red, green, blue, NIR*
Ground resolution	Adequate for UXO detection
Active sensor	None
Data format	*xyzρ* digitized from film
Suggested POC	Advanced Mapping Technologies, Inc. 1070 Sixth Ave. Suite 311 Belmont, CA 94002 (415) 637-0775 POC: John C. Eberhardt

**Exact spectral regions to be determined.*

4.2 Remote Minefield Detection System (REMIDS) (NIR and Thermal IR)

The REMID system (see table 3) was designed to remotely detect minefields from an airborne platform. The REMID system has an active sensor that operates in the NIR portion of the spectrum and a passive sensor that operates in the thermal IR portion of the spectrum. The active sensor uses a laser to illuminate the scene and measures reflectance and polarization differences. The passive sensor measures ε or apparent temperature differences in the scene. The data sets from both sensors are combined and processed to determine the presence of a minefield. Neither sensor requires the sun as an illumination source.

4.3 Hyperspectral Scanner (Visible to Far IR)

The data from hyperspectral scanners (see table 4) would be useful for spectral characterization of the signature of the background and surface UXO, not for direct use as a surface UXO detector. The visible and NIR information would be used to optimize the optical filters of the photographic system, based on the bands of optimum contrast between the UXO and the background. Alternatively, analysis of all the data may result in the choice of a number of selected bands from the visible to the far IR that could optimize UXO detection. These data would therefore allow the design of a multispectral sensor specialized for UXO detection. (Flanders [7] gives a general discussion of hyperspectral scanners.)

4.4 Proposed Laser Illuminator

New paints have been developed (see table 5) that use fluorescent dyes which, when stimulated with a laser of the proper frequency, can be made to glow at a characteristic wavelength [8]. The paints are currently being investigated for the purpose of tagging aircraft parts for later recovery after a plane crash. For future surface UXO remediation or for soft recovery of experimental ordnance, it is recommended that these new paints be investigated. Assuming the paints can be made to survive the harsh military environments, painted ordnance would be easy to spot when illuminated with a laser. Even partially buried or obscured ordnance could be spotted by this technique.

Table 3. Features of Remote Minefield Detection System (REMIDS).

Feature	Description
Sensor type	Thermal IR, NIR reflectance and polarization
Spectral bands	Far IR (8–12 μm) and 1.053 μm
Ground resolution	7.6 cm
Active sensor	NdYLF laser for polarization sensing
Data format	6 channels: 3 polarization, 1 reflectance, 1 laser diagnostic, and 1 thermal IR
Suggested POC	U.S. Army Corps of Engineers Waterways Experiment Station Vicksburg, Mississippi

Table 4. Features of hyperspectral scanner.

Feature	Description
Sensor type	Hyperspectral scanner
Spectral bands	Visible to far IR, broken into a number of separate spectral bands
Ground resolution	10 m typical
Active sensor	None
Data format	$xy\rho\lambda$ digitized format
Suggested POC	GER Corporation
	Environmental Research Institute of Michigan (ERIM)
	Jet Propulsion Lab

Table 5. Proposed laser illuminator.

Feature	Description
Sensor type	Laser illuminator
Spectral bands	Visible to mid-IR
Ground resolution	Fluorescent sensor dependent
Active sensor	Laser illuminator
Data format	xy

5. Conclusions

There are commercially available visible/IR systems that, with some modifications, should attain the resolution required for UXO detection. The main concern of UXO remediation, therefore, is not detection but rather discrimination from other objects in the scene. An investigation of the emissivity/reflectance characteristics of the soil, vegetation, and ordnance is required to aid in the analysis of target signatures and clutter rejection during the postprocessing of data. A database containing the emissivity/reflectance characteristics of the desert and/or UXO materials is required. Some preliminary optical measurements of a Yuma UXO test range are presently being made. The sensors involved are an airborne stereoscopic visible/IR camera, a thermal imager, and possibly, the remote mine detection (REMID) system. It is recommended that additional measurements be made (primarily the collection of hyperspectral data) and a full analysis of the data be performed before a final selection of an optical suite is made. If this data collection and analysis are undertaken early on, tremendous gains in the automatic recognition of targets can be achieved.

Acknowledgment

We would like to acknowledge the support given to this project by the Test and Evaluation Command and Yuma Proving Ground. Contributions from the Central Test and Evaluation Investment Program's Test Technology Development and Demonstration project, in part, enabled the collection and analysis of data and presentation of the results in this report.

References

1. Joseph Lintz, Jr., and David S. Simonett, editors, *Remote Sensing of Environment*, Addison-Wesley Publishing Company, Inc., Reading, Massachusetts (1976).

2. George J. Zissis, editor, *The Infrared and Electro-Optical Systems Handbook: Volume 1. Sources of Radiation*, SPIE Optical Engineering Press, Bellingham, Washington (1993).

3. John H. Ballard, Brian H. Miles, Raymond M. Castellane, and Daniel H. Cress, *Reflectance and Polarization Study Conducted During Standoff Minefield Detection Technical Demonstration, Fort Hunter Liggett, CA*, Waterways Experiment Station, Corps of Engineers, Technical Report EL-91-18 (December 1991).

4. W. L. Wolfe and G. J. Zissis, editors, *The Infrared Handbook*, Infrared Information Analysis (IRIA) Center, Ann Arbor, Michigan, 3rd printing (1989).

5. Richard D. Hudson, Jr., *Infrared System Engineering*, Wiley-Interscience, New York (1969).

6. *Infrared Imaging Systems Analysis*, Environmental Research Institute of Michigan, Ann Arbor, Michigan (1993).

7. David Flanders, *Hyperspectral Scanners Map Environments, Monitor Processes*, Photonics Spectra (April 1994), p 20.

8. *Laser Paint Assists in Search and Rescue*, Photonics Spectra, Laurin Publications (September 1994), p 21.

Distribution

Admnstr
Defns Techl Info Ctr
Attn DTIC-OCP
8725 John J Kingman Rd Ste 0944
FT Belvoir VA 22060-6218

OUSD(A&T/DTSENE/TFR
Attn J Bolino 3D1067
3110 Defense Pentagon
Washington DC 20301-3110

Hdqtrs Dept of the Army
Attn DAMO-FDQ MAJ M McGonagle
400 Army Pentagon
Washington DC 20310-0460

Test and Eval Mgmt Agency
Attn DACS-TE J Gehrig
200 Army Pentagon
Washington DC 20310-0200

US Army Environmental Ctr
Attn COL Uyesugi
Aberdeen Proving Ground MD 21010-5401

US Army Test & Evaluation Cmnd
Attn AMTE-CT-T J Schnell
Aberdeen Proving Ground MD 21005-5055

US Army Yuma Proving Ground
Attn STEYP-ES L Vanderzyl
Attn STEYP-TD-ATO A Hooper
Yuma AZ 85365

US Army Rsrch Lab
Attn AMSRL-CI-LL Tech Lib (3 copies)
Attn AMSRL-CS-AL-TA Mail & Records Mgmt
Attn AMSRL-CS-AL-TP Tech Pub
Attn AMSRL-SE-EE D Robinson (10 copies)
Attn AMSRL-SE-EE W Ruff (10 copies)
Adelphi MD 20783-1197

REPORT DOCUMENTATION PAGE

Form Approved
OMB No. 0704-0188

1. AGENCY USE ONLY *(Leave blank)*	2. REPORT DATE	3. REPORT TYPE AND DATES COVERED
	October 1997	Final, June 1994–November 1994

4. TITLE AND SUBTITLE

UXO Detection Using Optical Sensors

5. FUNDING NUMBERS

DA PR: AH16
PE: 6120A

6. AUTHOR(S)

Dale E. Robinson and William C. Ruff

7. PERFORMING ORGANIZATION NAME(S) AND ADDRESS(ES)

U.S. Army Research Laboratory
Attn: AMSRL-SE-EP
2800 Powder Mill Road
Adelphi, MD 20783-1197

8. PERFORMING ORGANIZATION REPORT NUMBER

ARL-MR-226

9. SPONSORING/MONITORING AGENCY NAME(S) AND ADDRESS(ES)

U.S. Army Test and Evaluation Command
Attn: AMTE-CT-T
Yuma Proving Ground, AZ 85365

10. SPONSORING/MONITORING AGENCY REPORT NUMBER

11. SUPPLEMENTARY NOTES

AMS code: 622120.H1611
ARL PR: 411911

12a. DISTRIBUTION/AVAILABILITY STATEMENT

Approved for public release; distribution unlimited.

12b. DISTRIBUTION CODE

13. ABSTRACT *(Maximum 200 words)*

Owing to cuts in the Defense Department budget, many military bases have been forced to close. Before these bases can be converted from military to civilian use, the unexploded ordnance (UXO) must be located and completely removed. The ordnance to be cleaned ranges from large-caliber rounds to small submunitions, which can be as small as 2 cm in diameter. In this report, we derive the basic theory necessary for the design of a UXO sensor operating in the visible to far-infrared wavelength regions. We then analyze several commercial off-the-shelf (COTS) sensors that could be used for UXO detection and present a few general conclusions on work required before a UXO sensor is fabricated.

14. SUBJECT TERMS	15. NUMBER OF PAGES
UXO, optical, sensors	25
	16. PRICE CODE

17. SECURITY CLASSIFICATION OF REPORT	18. SECURITY CLASSIFICATION OF THIS PAGE	19. SECURITY CLASSIFICATION OF ABSTRACT	20. LIMITATION OF ABSTRACT
Unclassified	Unclassified	Unclassified	UL

NSN 7540-01-280-5500

Standard Form 298 (Rev. 2-89)
Prescribed by ANSI Std. Z39-18
298-102